

# Drag Reduction using Innovative Design in Decelerating Duct of Marine Propeller

Md. Ayaz J. Khan<sup>\*1</sup>, Sanjay D. Pohekar<sup>2</sup>, Pramodkumar M. Bagade<sup>3</sup>

<sup>1</sup>Dept. of Mechanical Engg., Indian Maritime University, Tolani Maritime Institute, Pune-410507, India.

<sup>2</sup>Dept. of Mech. Engg., Symbiosis International University, Symbiosis Center for Research and Innovation, Pune-412215, India.

<sup>3</sup>Dept. of Mechanical Engg., Savitribai Phule Pune University, JSPM, Narhe Campus, Pune-411041, India.

ayazk@tmi.tolani.edu

**Abstract –** Reducing fuel consumption and carbon emissions with traditional propellers has become increasingly difficult in today's shipping sector. The current study aims to investigate the potential for reducing drag on marine propeller ducts using flow separation control. A nozzle is a hydrodynamically engineered duct that encircles the tip of a propeller's blade to control water flow better. The academic literature contains limited experimental and computational studies on the control of flow separation over hydrofoils. Also, the duct section with NACA hydrofoils is less studied. This study analyses the NACA4415 hydrofoil specifically for its practical application in decelerating duct designs. To control flow separation, dimpled surfaces are installed upstream of the separation point to energize the boundary layer. The current work uses computational fluid dynamics (CFD) to examine how “dimpled” surfaces affect the ducts' hydrodynamic properties. Ansys-Fluent was used to perform all transient simulations. NACA4415 performance is evaluated for lift, drag, pressure coefficient, vortex shedding, and Strouhal number at various angles of attack and flow conditions. It was discovered that the NACA4415 hydrofoil under consideration has a lower drag coefficient when its duct arrangement is decelerated and has a dimpled surface.

**Keywords:** NACA4415 Hydrofoil; Flow separation control; Marine decelerating duct

## INTRODUCTION

Shipping is a global industry requiring uniform global regulation. As per the report of the International Chamber of Shipping London (United Nations Framework Convention on Climate Change–UNFCCC, 2014), around 90% of world trade is carried by the international shipping industry.

The marine industry's top priorities today are cutting fuel usage and carbon emissions. Unconventional propulsion solutions for ships have been developed since it has become increasingly difficult to achieve this goal with conventional propellers. One such unconventional propulsion is by using ducted propellers, known as Kort nozzle. It is a duct or shroud with a hydrodynamic design that accelerates and directs water flow out of the marine propeller. A foil section circles the propeller in the nozzle, and the aft section of the nozzle tapers down to a diameter that is less than the propeller. The water flow can be made to accelerate (Fig.1a) or decelerate (Fig.1b) through the nozzles [1-2].

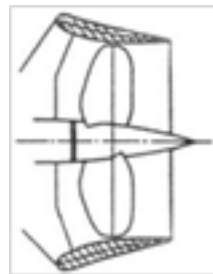


Fig.-1a: Accelerating duct

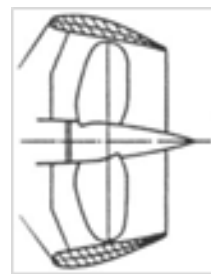


Fig.-1b: Decelerating duct

Towboats, ferries, and other maritime craft, such as diver propulsion vehicles (DPV), that need high maneuverability and low-speed operation typically use Kort nozzles. They are also utilized in applications like military and research vessels, where maximal thrust is necessary. The majority of ducted propellers manufactured following current commercial practice use accelerating ducts [1]. In ships, such as battleships, a decelerating duct is employed to lessen noise levels. Decelerating duct research data is typically less readily available in the literature. When compared to open propellers, Kort nozzles are 50% more effective, providing higher thrust per unit power [3,4]. At a speed of roughly 18.5 km/h (10 knots), they tend to lose their advantage over bare propellers. This speed can be increased by investigating flow separation control along the duct. The Marine Research Institute, Netherlands (MARIN) designed different nozzles such as the MARIN Nozzle No. 19A, 37, 24, and 22 for various thrust characteristics. However, the NACA hydrofoil sections for duct design are less explored. To improve the theoretical foundation for ducted propeller operation, Tsakonas and Jacobs [5] used the unstable lifting-surface methodology to explore the connection between the propeller and duct when operating in a non-uniform wake field. They used the results of this investigation to predict the geometry of the duct, propeller, and camber distribution of those sections.

#### **A. *Flow Separation Control***

The wall-bounded flow separates under specific steady or unsteady flow conditions. As long as the pressure difference along the surface remains constant, the fluid boundary layer that adheres to a solid surface keeps expanding. The thickness of this layer drastically increases when pressure is applied against the flow. The flow momentum within the layer is decreased due to

these conflicting pressures and shear forces. The expansion of this boundary layer will halt if any of these factors have a significant enough effect over a sizable surface area, a phenomenon known as flow separation [6]. According to Kundu [7], the critical Reynolds number depends on the leading edge's geometry, free stream instabilities, and surface roughness. Under these circumstances, the transition to turbulence is not instantaneous. As the name suggests, there is a transitional phase when the laminar flow first becomes unstable and then turbulent. Pai [8] assumes that the transition happens all at once to calculate the coefficient of friction in the turbulent boundary layer. According to Pai [8], given a smooth flat plate, the coefficient of friction is greater in a turbulent boundary layer than it is in a laminar boundary layer. Kundu [7] concurs that more macroscopic mixing in a turbulent flow causes turbulent boundary layers to provide more frictional resistance. If the plate abruptly changes from hydraulically smooth, the transition may be almost instantaneous.

Laminar flow can be disturbed by roughness components, which can lead to a turbulent transition much further upstream. Form drag (caused by pressure difference) and skin friction drag (caused by shear stress on the wall) make up the net drag force acting on the body. Streamlining the body reduces drag by decreasing the pressure difference on the surface [9]. The limit between forward and reverse flow in the layer, or the spot where the flow changes direction close to the wall, is sometimes referred to as the separation point. The wall shear stress is zero at the separation point. In comparison to a turbulent flow, a smooth boundary flow is naturally less stable and more likely to separate early. A backflow due to unfavorable pressure has been observed to occur downstream of this point, where flow acts in the opposite direction [10].

Separation control has received much attention from researchers as a way to shed light on basic flow mechanics and connect it to modern technology advancements. Hence investigation of separation has been the motive in the present research and is reported in the sections below.

## **BACKGROUND AND LITERATURE REVIEW**

During the past few years, substantial attempts have been made to significantly improve the efficiency of ship propulsion. However, detailed research on the flow separation control over hydrofoils is very limited both experimentally and computationally. The comparison of ducted propellers utilized for accelerating and decelerating flow was described by Razaghian et al. [11]. They looked into how the ducted propeller's length and angle affect hydrodynamics. Majdfar et al. [12–14] conducted studies that were comparable to these parameters. They demonstrated that increasing the duct angle increased force and torque while decreasing efficiency, especially at a low advance coefficient, using the 19A duct type and SST k- $\omega$  turbulence model. They used ducted propellers operating in oblique flow for their computational testing. Chamanara et al. [15] examined the effects of several turbulence models while studying the hydrodynamic characteristics of the Kort-nozzle. Caldas et al. [16] performed a computational analysis of numerous propeller ducts in open-water environments. The RANSE model was utilized to quantitatively investigate various propeller forms with configurable pitch.

Celik et al. [17] looked at the best duct geometry for a passenger ferry. The performance of various duct sections was evaluated, as well as the optimum duct layout for the Kort-nozzle propeller. Yu et al. [18] performed a numerical analysis of the ducted-nozzle

propellers in open-water test conditions. The impact of duct shape on the thrust performance of ducted propellers was documented by Krzysztof et al. [19].

### **A. Literature Gap and Objective of Present Work**

The NACA4415 aerofoil was primarily designed for low-speed applications, including wings or foils that glide underwater - hydrofoils. To reduce drag and enhance speed and efficiency, hydrofoils are used to elevate boats or other marine vehicles out of the water. A thorough review of the literature revealed that NACA4415 is the least used hydrofoil section for ducted propellers. Also, the flow separation control on hydrofoils is still less explored. In addition to examining the dynamics of fluid flow separation, pressure, velocity distribution, and lift and drag forces acting on the duct, this study primarily examines how well NACA4415 performs as a duct section.

The current work first investigates fluid characteristics for the chosen duct type, duct angle, and drag coefficient at different Reynolds Numbers. Later a flow separation control was analysed with a dimpled curvature at 80% chord length. Thus, the major goal of the current work is to explore the effect of flow separation control such as dimpled surface on NACA4415 hydrofoils for the marine decelerating duct section using CFD analysis.

## **METHODOLOGY**

To analyze the hydrodynamic performance of aerofoils at various angles of attack, researchers frequently use computational fluid dynamics (CFD) models or wind tunnel experiments. The fluid flow separation, pressure distribution, velocity contours, and lift and drag coefficients of the aerofoil may all be studied in great detail using these methods. The mesh on which to run the computations is an important consideration when executing CFD simulations with ANSYS-FLUENT.

The grid must possess high-quality metrics, such as orthogonality and skewness, to accurately capture the fluid flow characteristics surrounding the aerofoil. Additionally, the grid should be sufficiently refined to represent these features precisely. Bagade et al. [20] have highlighted the significance of orthogonality. The lift and drag coefficients were derived using computational fluid dynamics (CFD) study and subsequently compared to experimental data. Steady-state and transient analyses were conducted to mimic the flow over a NACA4415 aerofoil at various angles of attack.

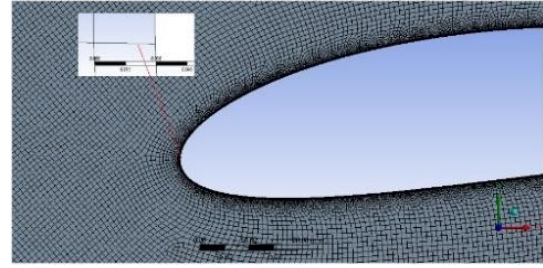
#### A. Geometry – Foil Section and Fluid Domain

In the present work, the NACA-4415 is analyzed for the Kort-nozzle decelerating duct section using computational fluid dynamic simulations. The inlet (upstream) and outlet (downstream) boundaries were taken as 12 and 28 times the chord length, respectively.

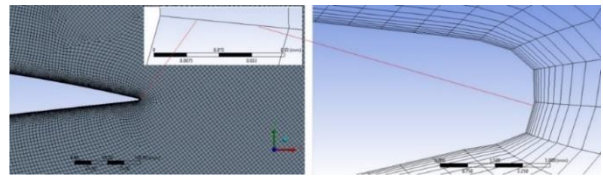
#### B. Mesh – Foil Section and Fluid Domain

The degree of concordance between CFD findings and actual data can be affected by a variety of factors, including mesh or grid resolution, turbulence modeling, and experimental errors. Simulations using very fine grids are required to effectively resolve the boundary layer and capture the complicated flow features near the hydrofoil surface. To perform grid sensitivity studies to determine the appropriate grid resolution, the simulations were run with different grid sizes, and the results were compared to see if there was a significant change in the computed flow variables such as lift and drag coefficients. The use of CFD simulations, along with fine grids and good-quality metrics, can provide valuable insights into the hydrodynamic performance of NACA4415. A nearly orthogonal grid was generated for the present numerical investigation following the importance of grid metrics [20]. Fig. 2 (a) and (b) show a zoomed view of the grid near the leading and trailing

edge of the hydrofoil. It can be seen that a very fine grid is used near the hydrofoil surface, while an orthogonal grid is used in the vicinity of the hydrofoil.



(a) Grid near the leading edge of the hydrofoil



(b) Grid near the trailing edge of the hydrofoil

Fig. 2 a,b: Details of the grid around the hydrofoil with inflation layers.

Fig. 3 a,b, and Fig. 4 show the wall and mesh resolution details near the dimpled region. A fine grid is generated using 921038 elements.  $y^+$  at the airfoil surfaces is  $y^+_{\min} = 0$  and  $y^+_{\max} = 1.59$ . The minimum and maximum cell wall distance is 0.0129 mm and 0.0154 mm. The grid metrics, fluid domain size and shape, mesh independency, aspect ratio,  $y^+$  value, orthogonality, and grid skewness are considerably good for the present investigation.

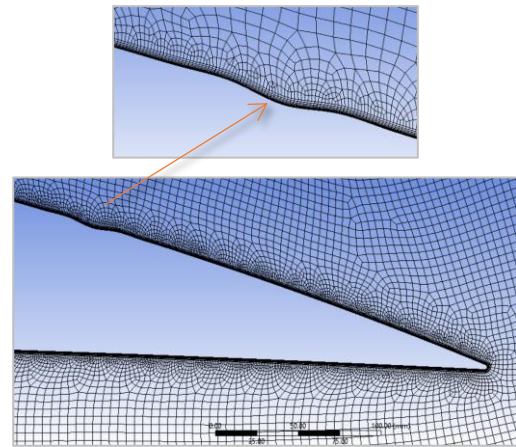


Fig. 3a: Grid around 'dimple' region

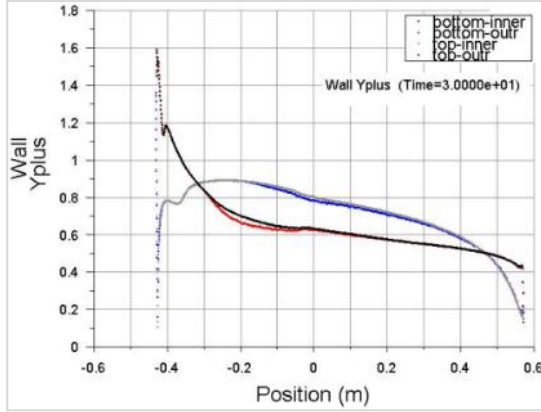


Fig. 3b: Grid resolution near the surface

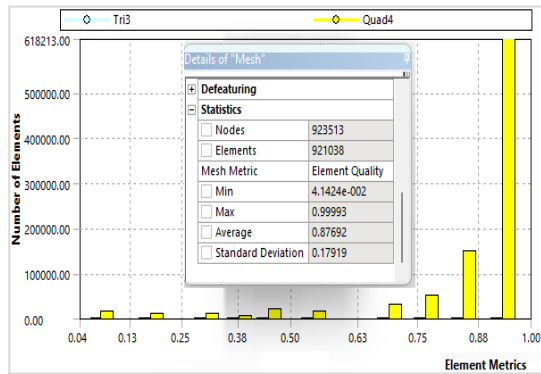


Fig. 4: Mesh quality details

### C. Boundary Conditions

The following boundary conditions (Table 1) are applied during simulations. Fig.5 shows the computational domain with boundary conditions for the duct configuration. The viscous-turbulent  $k-\omega$  SST is employed for the present computation as it provides an acceptable level of accuracy in unsteady flow predictions [21].

Table 1.

Inlet:	Velocity-inlet
Outlet:	Pressure-outlet
Models and Materials:	Fluid-Water
Viscosity of fluid=	0.001 Pa.s
Density of fluid=	1000 kg/m <sup>3</sup>
Models -Viscous-Turbulent:	$k-\omega$ SST
Problem Setup:	Pressure Based
Reynolds Number =	$1 \times 10^6$ , $2 \times 10^6$ and $5 \times 10^6$

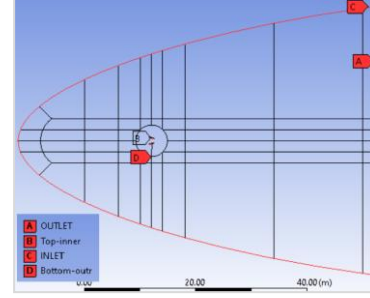


Fig.5.: Computational domain with boundary condition

## RESULTS AND DISCUSSIONS

### A. Investigation of Hydrodynamic Performance of a Single Hydrofoil

The NACA 4415 hydrofoil is analyzed for a range of angle of attack ( $-6^\circ < \alpha < 12^\circ$ ). Fig. 6 shows the validation plot comparing the experiment and current simulation results of the pressure coefficient at 0.15 degrees of angle of attack.

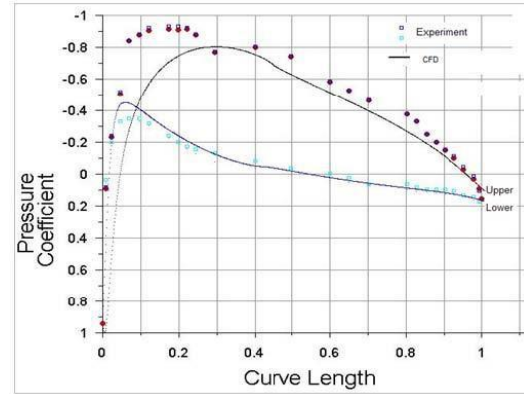


Fig. 6: Pressure coefficient distribution at  $\alpha = 0.15^\circ$

Fig. 7a and Fig. 7b show the drag and lift coefficients. The results obtained are in strong accordance with the experimental results of Hoffman [22] and [23]. It is noted that the increase in the drag values is insignificant in the range of  $-4^\circ \leq \alpha \leq 4^\circ$  angle of attack. This suggests that till  $\alpha = 4^\circ$ , the drag penalty will be minimal, while for higher duct angles ( $\alpha_d$ ), larger drag forces will act on the hydrofoil surface, affecting the overall efficiency.

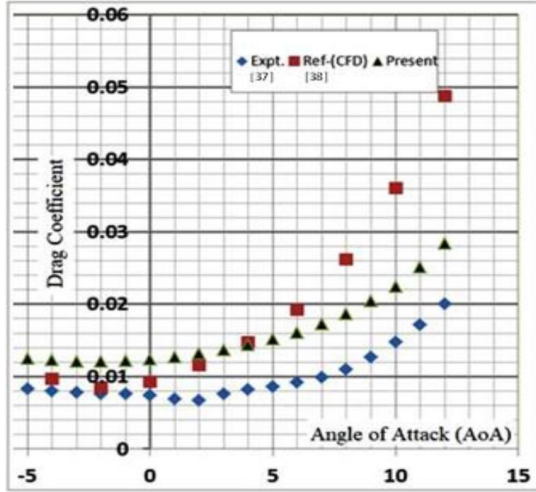


Fig. 7a: Drag coefficient, ( $C_d$ )

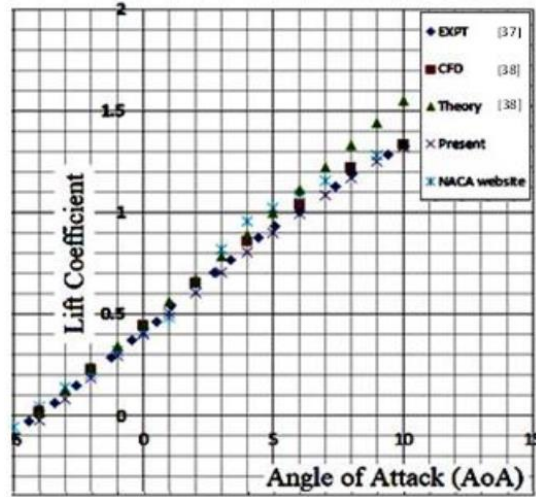


Fig. 7b: Lift coefficient, ( $C_l$ )

### B. Investigation of the Effect of Dimple on the Duct Profile

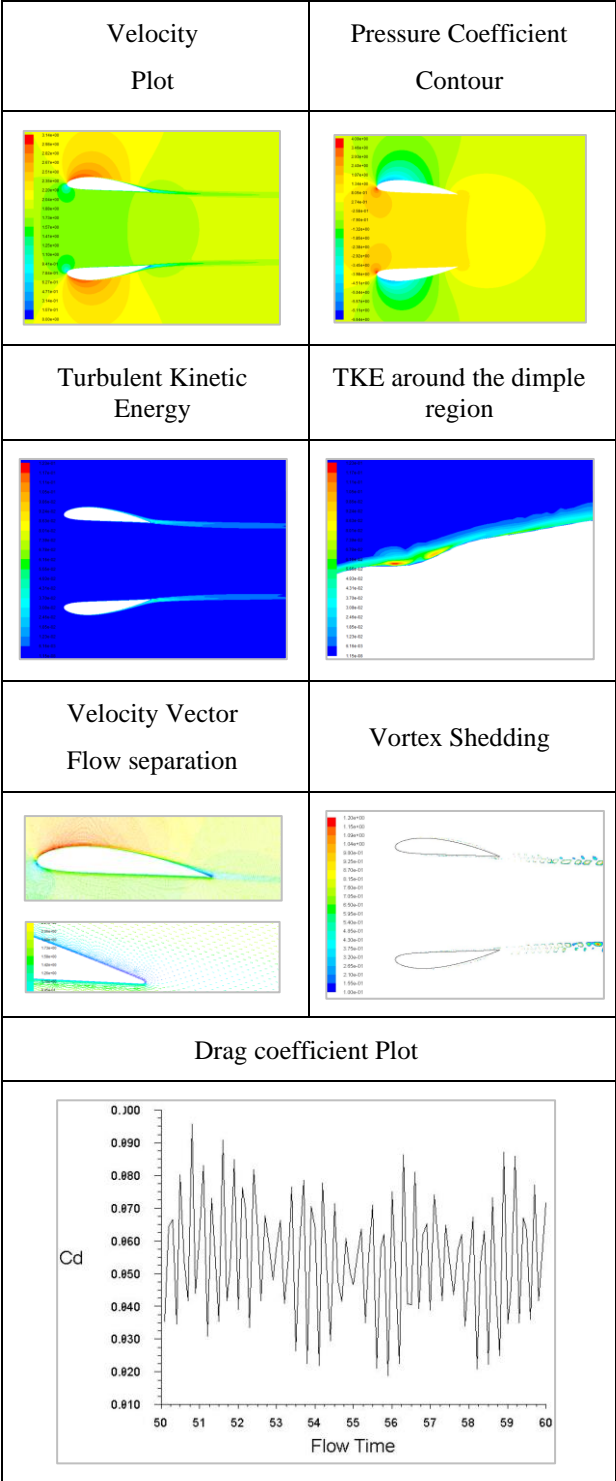
The following analyses the analytical relationship for designing the decelerating duct section using NACA-4415 hydrofoil. The preliminary stage was to develop the solution to a turbulent flow problem over a 2-D configuration for  $0^\circ \leq \alpha \leq 10^\circ$  duct angle. Three combinations were used in grid dependence research to achieve higher cell quality. Table 2 shows the post-processing results at one of the flow conditions ( $Re=2 \times 10^6$ ) for 0, 5, and 10-deg duct angles. Here different flow characteristics are compared.

Table 2: Post-processing

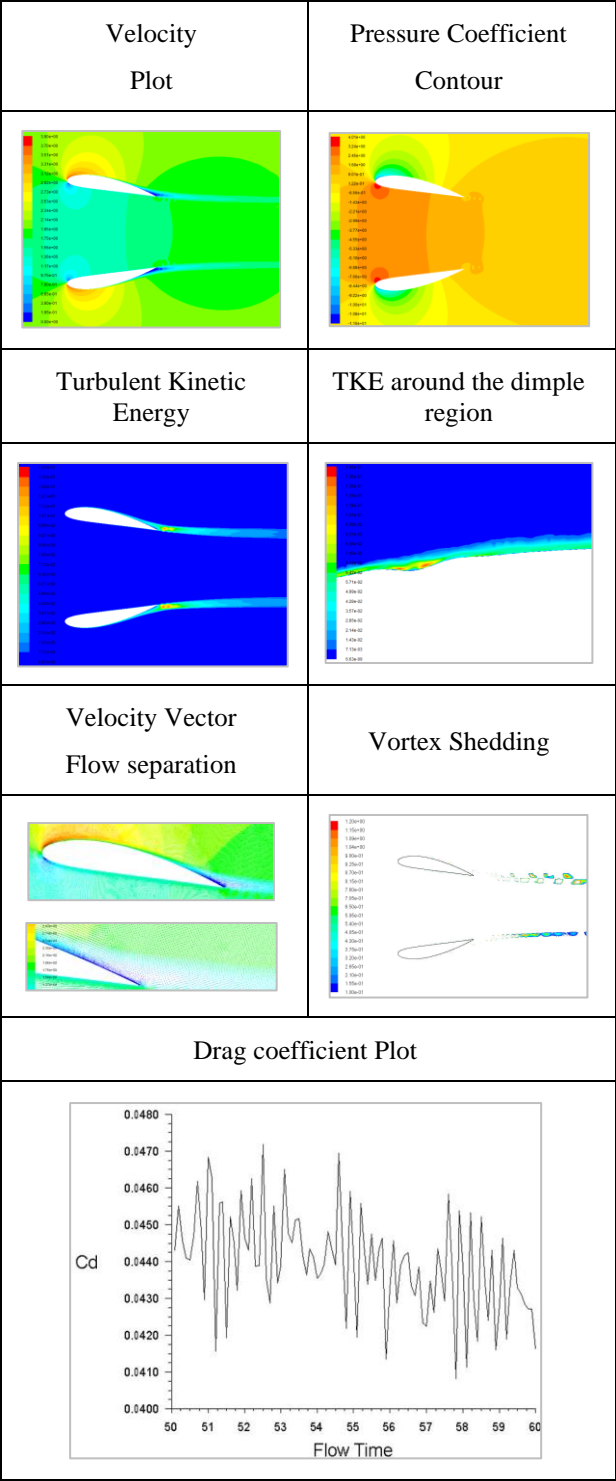
Duct Angle : 0 deg	
Velocity Plot	Pressure Coefficient Contour
Turbulent Kinetic Energy	TKE around the dimple region
Velocity Vector Flow separation	Vortex Shedding
Drag coefficient Plot	



Duct Angle : 5 deg



Duct Angle : 10 deg



### C. Investigation of the Effect of Dimple on Drag Coefficient

The results of a transient analysis for the drag coefficient of the decelerating duct at several Reynolds numbers and at various duct angles are shown in Figs. 8a, b, and c. The analysis is done for three sets of Re ( $1 \times 10^6$ ,  $2 \times 10^6$  and  $5 \times 10^6$ ) and 0 to 10 degrees duct angles. The discussion of key conclusions gained from these plots follows.

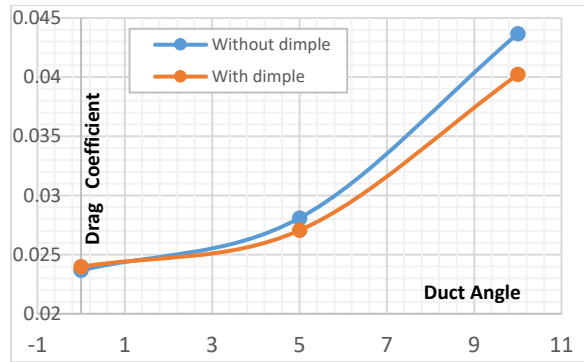


Fig. 8a: Drag Coefficient at Re 1e6

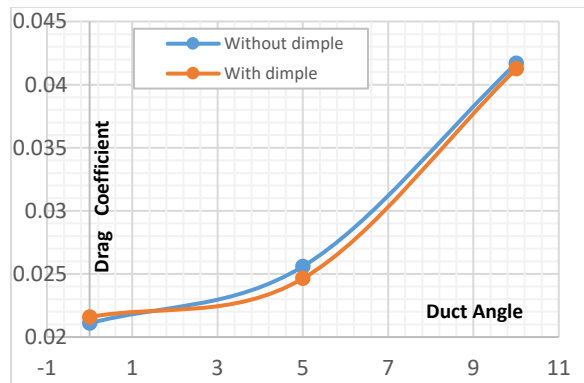


Fig. 8b: Drag Coefficient at Re 2e6

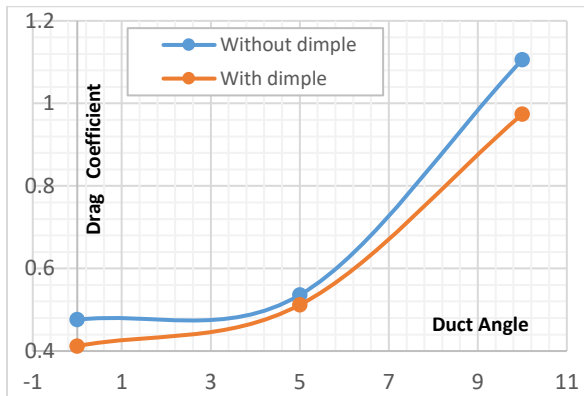


Fig. 8c: Drag Coefficient at Re 5e6

### D. Inferences on Result Data

- Flow separation control involves energization of the boundary layer upstream of the separation point by installing vortex generators, dimpled surfaces, and wall suction. In all the above plots, the drag coefficients ( $C_d$ ) for values at  $0^\circ$  to  $10^\circ$  duct angle for decelerating duct under unsteady flow conditions show that a decelerating duct with a 'dimple' produces lesser drag.
- Flow separation can occur on the surface of the marine nozzle, particularly near the diverging section leading to a reduction in propeller efficiency. Depending on the particular situation and the desired result, several alternate techniques can be used to manage flow separation. One typical method to encourage smoother flow and lessen turbulence is to alter the geometry of the object or surface in question. Utilizing active flow control methods, such as fluid injection or suction, is another strategy to prevent separation.
- The present study aims to understand analytical relationships for designing the marine nozzle duct section using NACA-4415 hydrofoil. The analysis was done for a range of duct angles. The objective was to establish the effect of dimples on the drag coefficient. The standard CFD model and PISO algorithm were adopted for transient analysis. The velocity, pressure distribution, vortex shedding, wall shear stress, and flow separation on the hydrofoil surface at different duct angles, along with the effect of increasing Reynolds number, were studied.



## CONCLUSION

For the marine nozzle, the drag force acting on the hydrofoil section is oriented in the direction of ship motion; thus, it aids the thrust produced by the propeller. Hence an optimum duct angle is of utmost importance to explore. The present work investigates the effect of the Reynolds number on the hydrodynamic parameters of the NACA4415 hydrofoil at various duct angles of the marine nozzle. Further, the work is extended to explore the flow separation control by making dimples at 80% chord length where the flow velocity is usually maximum.

The most important findings of the existing research are as follows:

- A total of 18 sets of configurations were investigated (0, 5, and 10-degree duct angles at Re's  $1e6$ ,  $2e6$ , and  $5e6$ ). The dimple on the hydrofoil profile energizes the boundary layer upstream of the separation point, reducing the net drag coefficient. At 10 degrees of duct angle, the flow separation control by profile with dimple shows a significant contribution to drag reduction.
- For marine nozzles with a duct angle greater than 5 degrees, a flow separation control mode such as the dimple used in current work will significantly help in net drag reduction and hence fuel consumption.

### *Scope for Future Work*

For particular vessel types and operational conditions, researchers may investigate novel duct forms and arrangements to enhance duct performance. For instance, the 'RICE' nozzle has a lower drag coefficient than a standard MARINE-19A series nozzle.

## REFERENCES

- [1] Carlton J. S., Marine Propellers and Propulsion, Second Edition, Elsevier Publications, (2007).
- [2] Celik F., Donguland A. Arikian Y., Investigation of optimum duct geometry for a passenger ferry, IX HSMV Naples, (25-27 May 2011).
- [3] Stipa L., Experiments with Intubed Propellers, L'Aerotechnica, pp 923-953, Aug.1931, Translated by Dwight M. Myner, NACA TM 655, (Jan. 1932).
- [4] Stipa L., On the use of Propellers of Various Types, reprinted from L' Aerotechnica, Vol. 8 (3), March 1932, translated by A. A. Fanelli for the Aerophysics department of Mississippi State College, (1956).
- [5] Tsakonas, S., Jacobs, W. R., Propeller Loading Distributions, Defence Technical Information Center, Accession Number: AD0682483, (1968), <https://apps.dtic.mil/sti/citations/AD0682483>
- [6] Gad-el-Hak M., Bushnell D.M., Separation Control: Review, Journal of Fluids Engg., 113:5–30, (1991).
- [7] Kundu, Pijush K. and Cohen, Ira M., 'Fluid Mechanics' Elsevier Inc., Ed. 4, pp 104-105, 340-400, (2008).
- [8] Pai, Shih-I, 'Viscous Flow Theory, II – Turbulent Flow', D. Van Nostrand Company, Inc., pp 60-114, (1957).
- [9] Hermann Schlichting, Klaus Gersten, Boundary Layer Theory, Springer Publ., (2017).
- [10] Viswanath P. R., Some thoughts on separation control strategies, Sadhana, Vol. 32, (1 & 2), 83–92, (2007).
- [11] Razaghian A. H., Ghassemi H., Numerical analysis of the hydrodynamic performance of the accelerating and decelerating ducted propeller, Scientific Journals of the Maritime University of Szczecin, Vol. 48, (2016).

- [12] Majdfar S., Ghassemi H., Forouzan, H., Hydrodynamic prediction of the ducted propeller by CFD solver, *Journal of Marine Science and Technology*, Vol. 25 (3), pp. 268-275, (2017).
- [13] Majdfar S., Ghassemi H., Forouzan H., Hydrodynamic Effects of the length and angle of the ducted propeller, *Journal of Ocean, Mechanical and Aerospace Science and Engineering*, Vol.25, (2015).
- [14] Majdfar S., Ghassemi H, Calculations of the hydrodynamic characteristics of a ducted propeller operating in oblique flow, *Ship Science and Technology*, Vol. 10(20), pp. 31-40, (2017).
- [15] Chamanara M., Ghassemi H., Hydrodynamic characteristics of the Kort nozzle propeller by different turbulence models, *American Journal of Mechanical Engineering*, Vol. 4 (5), pp 169-172, (2016), doi: 10.12691/ajme-4-5-1.
- [16] Caldas Alejandro, Meis Marcos, and Sarasquete Adrián, CFD validation of different propeller ducts on open water condition, 13th Numerical Towing Tank Symposium; Duisburg Germany, (October 2010).
- [17] Celik F., Donguland A. Arian Y., Investigation of optimum duct geometry for a passenger ferry, IX HSMV Naples, (May 2011).
- [18] Long Yu, Martin Greve, Markus Druckenbrod, Moustafa Abdel-Maksoud, Numerical analysis of ducted propeller performance under open water test condition, *Journal of Marine Science and Technology*, (2013).
- [19] Krzysztof Szafran, Oleksandr Shcherbonos, Dariusz Ejmocki, Effects of duct shape on ducted propeller thrust performance, *Transactions of the Institute of Aviation*; No.4 (237), pp. 84-91, Warsaw, (2014).
- [20] Bagade, P.M., Bhumkar, Y. G., Sengupta, T. K., An improved orthogonal grid generation method for solving flows past highly cambered aerofoils with and without roughness elements, *Computers & Fluids*, 103, 275–289, (2014).
- [21] Belhenniche Samir. E, Amounallah Mohammed, Imine Omar, Celik Fahri, Effect of Geometric Configurations on Hydrodynamic Performance Assessment of a Marine Propeller, *Brodogradnja / Shipbuilding*, Vol. 67 (4), 31-48, (2016), doi.org/10.21278/brod67403.
- [22] Hoffmann, M. J., Reuss Ramsay, R., Gregorek, G. M., Effects of Grid Roughness and Pitch Oscillations on the NACA 4415 Airfoil, *NREL/TP-442-7815*, (1996)
- [23] <https://chart-studio.plotly.com/~amruthwo/43.embed>
-